Integrated Wi-Fi Sensing and Communication for Soil Moisture Monitoring

Henrique Freire da Silva[1], **Bruno de Carvalho Albertini**[1], **Cíntia Borges Margi**[1]

[1] Departamento de Engenharia de Computação e Sistemas Digitais
Universidade de São Paulo (USP) – São Paulo, SP – Brazil

{hfreire,balbertini,cintia}@usp.br

Abstract. *Soil moisture monitoring is essential for efficient irrigation and crop management in precision agriculture. Conventional methods rely on manual sampling or dedicated sensors, which limit large-scale deployment due to cost and infrastructure requirements. RF-based sensing offers an alternative by exploiting changes in signal amplitude and phase caused by soil dielectric properties. This work evaluates soil moisture sensing using Wi-Fi on resource-constrained ESP32 devices in a laboratory and an in the field. Our study takes into consideration the distance between devices, and the CSI amplitude and phase. Confined experiments introduced bias in channel metrics, while field tests revealed sensing limitations with increasing range.*

1. Introduction

According to the United Nations, the global population is expected to reach 10.3 billion by the mid-2080s and stabilize near 10.2 billion by the end of the century [United Nations nd]. This growth intensifies the demand for food, water, and energy. Agriculture must therefore adopt systems that use resources efficiently and sustainably.

Precision agriculture applies data analytics to sensor data collected through Internet of Things (IoT) networks to optimize inputs and decisions at field scale. In this context, tracking soil moisture plays a crucial role in maintaining crop health, maximizing yield, and managing water and weather impacts efficiently. It enables precise irrigation control and supports responsible water management [Hardie 2020, Rasheed et al. 2022].

Large-scale deployment of conventional soil moisture sensing remains costly. Laboratory gravimetric methods require soil sampling and analysis, while in-field sensors trade off spatial resolution, penetration depth, and temporal coverage. Field installation increases labor and maintenance effort, and data collection requires communication infrastructure. These constraints limit dense deployments in large or remote agricultural areas and hinder their widespread adoption [Kashyap and Kumar 2021].

Radio-Frequency (RF)-based sensing explores the interactions of wireless signals with the environment. The propagation medium affects the electromagnetic waves through its dielectric properties and geometry, altering the signal amplitude and phase. The electrical permittivity and conductivity of soil are primarily related to moisture content and salinity [Ding and Chandra 2020]. As signals traverse the soil, the perceived propagation channel corresponds to these soil variables.

The Integrated Sensing and Communication (ISAC) paradigm introduces sensing functions into communication infrastructure, sharing spectral, temporal, and hard-

ware resources. Unlike traditional sensing architectures, ISAC jointly designs sensing and communication services, eliminating redundancies and reducing associated costs [Cui et al. 2021].

The adoption of wireless communication standards, such as BLE [Hänel and Kaiser 2024], RFID [Wang et al. 2020], LoRa [Kiv et al. 2021], and Wi-Fi [Hernandez et al. 2021, Ding and Chandra 2020, Ding et al. 2024], enables the reuse of existing infrastructure and link metrics to infer environment information [Chen et al. 2023]. Wi-Fi is particularly valuable, providing Channel State Information (CSI) that captures attenuation and phase shifts in each Orthogonal Frequency-Division Multiplexing (OFDM) subcarrier [Hernandez and Bulut 2023]. This information enhances the ability to detect soil dielectric variations using widely available commercial devices

However, many Wi-Fi sensing studies for soil monitoring rely on traditional network interface cards and Multiple-Input Multiple-Output (MIMO) systems [Ding and Chandra 2020, Ding et al. 2024]. Experiments often occur in confined spaces with controlled irrigation setups. Additionally, the experimental design focuses exclusively on the sensing task, disregarding communication requirements and their implications for ISAC architectures.

In this work, we investigate the integration of sensing and communication for soil moisture systems using resource-constrained devices. We propose a system architecture using ESP32 devices to evaluate the amplitude and phase of CSI on soil, both in laboratory and field conditions. Experiments in confined environments induced biases in the channel metrics, while field test with ranges above 33 cm showed low sensing rate. Finally, soil moisture affects signal amplitude and phase in complementary ways, with correlation coefficients of 0.55 and -0.58, respectively.

2. Related Work

The potential to reuse communication infrastructure for sensing drives substantial research interest in ISAC [Chen et al. 2023]. In practice, many implementations separate sensing and communication by allocating non-overlapping resources. Time-division schemes that schedule sensing and communication in distinct time intervals are particularly common and practical to implement [Cui et al. 2021].

Wi-Fi transmissions rely on OFDM at the physical layer, which divides the channel into narrowband subcarriers and embeds a known preamble at each frame for channel estimation [IEEE 2021]. Receivers extract CSI from the preamble by comparing received symbols with expected symbols. The resulting complex per-subcarrier gains supply amplitude and phase measurements across frequency, revealing fine-grained variations in the propagation channel [Hernandez and Bulut 2023].

The propagation environment shapes these CSI measurements: radio waves interacting with materials undergo reflection, refraction, scattering, and absorption. The resulting amplitude and phase changes depend mainly on the dielectric properties of the medium. Higher permittivity increases signal delay and shortens the wavelength, while higher conductivity increases attenuation. Variations in permittivity and conductivity therefore alter the received signal across frequency and time, directly influencing the observed CSI [Hernandez et al. 2021].

Soil type, salinity and volumetric water content modify the medium response to RF signals: water exhibits higher permittivity than dry soil, so even modest changes in moisture can produce measurable shifts in the propagation time of signals [Ding and Chandra 2020]. Empirical relations, such as the Topp model [Topp et al. 1980], map permittivity to volumetric water content under certain soil type and temperature assumptions. These models, when combined with site-specific calibration or prior knowledge about soil composition and temperature, enable the translation of observed CSI amplitude and phase variations into quantitative soil moisture estimates, linking radio propagation physics to practical environmental monitoring.

Several studies have explored these principles for soil monitoring using wireless signals. Ding and Chandra [Ding and Chandra 2020] employ a MIMO system at 2.4 GHz. They place a transmitter above ground and bury receiving antennas to capture Time-of-Flight (ToF) and signal attenuation. Their approach separates apparent permittivity and conductivity, estimating soil moisture and salinity around the antennas. The authors compare their metrics to results from software-defined radios with larger bandwidths and demonstrate similar outcomes. However, the study does not address communication mechanisms or integration with field monitoring systems. The network interface cards used are not compatible with microcontroller-based platforms and require dedicated hardware for sensor nodes.

Hernandez et al. [Hernandez et al. 2021] propose an underground Wi-Fi mesh for soil moisture monitoring, texture classification, and inter-node distance estimation, reporting accuracies of up to 97%, 90%, and 99%, respectively. The authors use ESP32 devices with a single antenna, keeping hardware cost-effective. Despite promising results, the moisture experiments were conducted only under laboratory conditions. The study presents sensing–communication integration at a conceptual level and lacks a field implementation and protocol details required to sustain both functions on the same infrastructure.

Nguyen et al. [Nguyen et al. 2023] show that water infiltration selectively affects OFDM subcarriers. They conducted experiments at 5 GHz using inexpensive devices and observed that some subcarriers are more sensitive to moisture changes than others. This selectivity enables finer discrimination of infiltration dynamics. However, the experiments remain restricted to laboratory setups with homogeneous soil moisture, small containers, and shallow measurement depths.

Overall, Wi-Fi sensing studies on soil monitoring span both MIMO and Single-Input Single-Output (SISO) radio configurations. MIMO approaches exploit multiple antennas to increase spatial resolution, but their hardware and processing requirements limit their applicability in microcontroller-based platforms. Consequently, studies that rely on microcontrollers typically adopt SISO configurations and conduct experiments in laboratory settings, often using confined containers that restrict environmental variability. In addition, these studies generally focus exclusively on sensing and overlook the communication requirements inherent to ISAC architectures. This separation limits the understanding of how sensing performance interacts with communication constraints in practical deployments. Our study addresses this gap by investigating a SISO implementation suitable for microcontrollers while considering sensing and communication jointly within an ISAC framework.

3. Communication and Sensing Architecture

Traditionally, the cost of a sensing device includes the sensor itself, a microcontroller, and a communication radio. In addition, farmers must bear the costs associated with installing and maintaining the network infrastructure required for device operation. The cost of single-depth sensor nodes with LoRaWAN connectivity usually range from U$100 to U$700 [Elshikha 2024]. Wi-Fi–based sensing for soil moisture estimation has emerged as an alternative to this approach. By using Wi-Fi signals for sensing, the same radio hardware also handles data communication. As a result, the device cost is reduced to the microcontroller and the radio interface, when the latter is not already integrated into the system. ESP32 Systems on Chip (SoCs) with Wi-Fi radios cost from $U2 to $U5 [Espressif Systems 2026]. The use of multiple devices to sense the same Wi-Fi stream could further reduce the need for LoRa modules to a single device that aggregates sensor data in this network.

Accurate soil moisture estimation requires Wi-Fi signals to propagate predominantly through the soil. Therefore, the sensing antennas must be buried at the depth of interest. In contrast, long-range data transmission requires antennas positioned above the ground surface. To address this constraint, the proposed system separates the sensing and communication functions using dedicated antennas: the sensing antenna remains buried in the soil, while the communication antenna is placed above ground near the microcontroller. These antennas are time multiplexed to accommodate the connectivity constraints of sensing platforms such as the ESP32, allowing for a single radio per node. Other forms of multiplexing require either multiple radios operating at different channels (spectral division) or MIMO-capable radios (spatial division).

A single node cannot perform Wi-Fi sensing independently. Therefore, we organize the devices into groups. Each group includes one initiator (TX) and multiple sensor nodes (RXn). The initiator generates periodic Wi-Fi transmissions, while the sensor nodes capture these signals to estimate CSI/Received Signal Strength (RSSI) and infer the soil conditions. Figure 1 illustrates the proposed sensor group architecture. A single radio alternates between the two antennas as needed, aligning the design with ISAC principles.

Each sensor node integrates a microcontroller with a Wi-Fi radio, an RF switch for antenna selection, and a capacitive soil sensor used as a reference measurement. The microcontroller manages antenna selection, schedules sensing and low-power periods, aggregates measurements, and handles data transmission.

The system operates as follows. After power-up, all devices select the communication antenna and attempt to connect to the configured Wi-Fi network (i). Communication and sensing share the same channel, therefore all nodes in the group operate on a common channel. Once the initiator connects, it begins periodic sensing transmissions that include two fields: a sequence identifier and a baseline moisture reading obtained from its reference sensor (ii). The sequence field enables temporal alignment across sensor nodes, while the baseline measurement provides contextual information about soil conditions in the sensing region.

After joining the network, each sensor node switches to the sensing antenna, enables channel metric collection, and waits for the next initiator frame. Upon reception, the node records the corresponding CSI and RSSI values and performs a reference soil

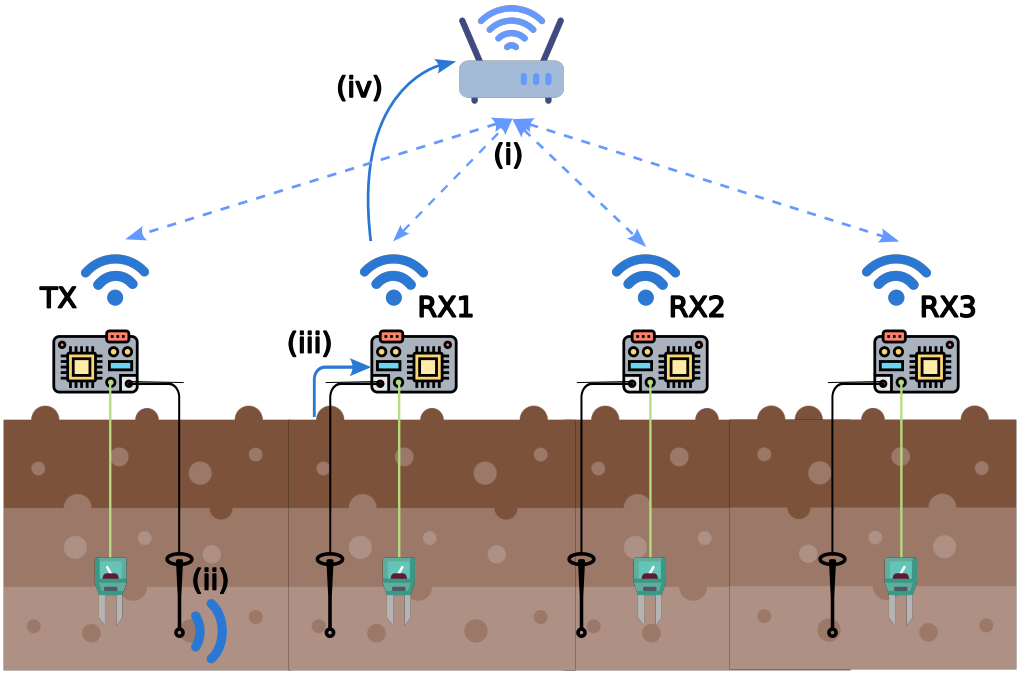

Figure 1. Proposed sensing architecture. Icons made by Eucalyp, SlamLabs, Those Icons, and Umeicon from www.flaticon.com.

moisture measurement (iii). The node then enters a low-power state by reducing the processor and peripheral clocks and disabling the Wi-Fi radio until the next sensing cycle. Sensors accumulate measurements in memory and, once the transmission buffer is full, switch back to the communication antenna to transmit the collected dataset using the Carrier Sense Multiple Access with Collision Avoidance (CSMA/CA) protocol (iv). Channel metric collection remains disabled during transmission, after which the node resumes the sensing cycle.

4. Method

We first reproduced typical laboratory experiments that rely on soil-filled containers instead of field tests. We focused on spatial resolution, specifically how localized moisture variations between two devices affects the CSI measurement. We then conducted a field experiment to evaluate sensor range and the architecture proposed in Section 3.

4.1. Laboratory Experiment

For our tests, we used a plastic container. We placed a 2 cm layer of a commercial potting mix on the bottom and leveled the surface, then wrapped two ESP32 modules in plastic film for moisture protection and fixed them to opposite edges of the container, 30 cm apart. We filled the container with an additional 8 cm of soil to fully cover the devices. Figure 2.a presents the setup used.

One module acted as the station (STA) and the other as the access point (AP). The STA transmitted ICMP Echo requests at 20 Hz for 180 seconds, and the AP replied to each request. We used the returned packets to estimate CSI and RSSI at the STA. We also limited transmit power to 10 dBm on both devices, given the container size.

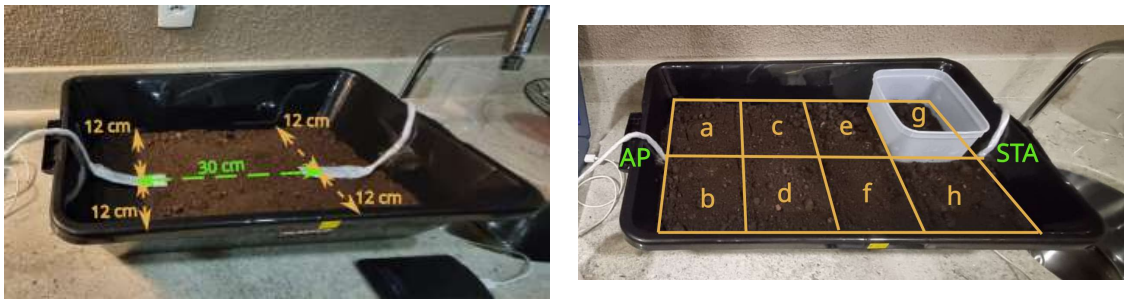

(a) Device position in container. (b) Watering grid.

Figure 2. Laboratory experiment setup.

We initially recorded reference CSI and RSSI for the resting moisture. We then overlaid a 4×2 grid of cells, each 12.5×14 cm, on the soil surface. Figure 2.b illustrates the cell identifiers and orientation relative to the AP and STA. We irrigated the cells in alphabetical order, adding 100 mL of water to a single cell, waiting for stabilization, and recording CSI and RSSI within the measurement window. We repeated this sequence three times per cell, increasing local moisture in steps up to a cumulative 2.4 L and producing a heterogeneous moisture pattern across the grid.

4.2. Field Experiment

Given the architecture in Figure 1, we implemented a four-node group (three sensors and one initiator) operating at 100 ms intervals (10 Hz). We selected this sampling rate to capture the gradual medium changes associated with water percolation. We buried the sensing antennas 35 cm deep and aligned them on a common reference. The setup places sensor nodes at 33, 66, and 100 cm from the initiator. We used ESP32-C6 modules (integrated Wi-Fi radio and antenna) at 2.4 GHz.

For field operation we produced three artifacts per sensing node: a reference soil moisture sensor, an external antenna adapted for underground use, and a protective enclosure. We also prepared a USB-C power cable for each node. The sensing antenna consists of a rigid copper wire with appropriate cables and connectors, and the reference instrument comprised a commercial capacitive probe with an extension cable for field placement.

The reference soil moisture sensor is an adaptation of a commercial capacitive sensor for field use. We enclosed its electronics in a two-part 3D-printed housing, exposing only the probe and an access point to the terminals, and sealing the enclosure with hot glue and silicone. We soldered the sensor leads to a four-conductor jacketed cable (24 AWG), sized to 1 m for installation convenience, and applied self-fusing tape over all joints to prevent moisture ingress.

The external antennas are monopoles made of a rigid copper wire cut in lengths of 3.08 cm (a quarter of wavelength for 2.4 GHz) and soldered into a type-N connector. They are housed inside a PVC tube with removable end caps, fixed by the coax entry with hot glue, and applied silicone sealing to prevent water ingress.

(a) Open pits. (b) Antennas and sensors positioned. (c) Devices buried.

Figure 3. In-field device deployment.

We built a 20 m power harness fed from a single 5 V switched mode power supply, using 22 AWG two-core cable dimensioned for up to four ESP32 modules and branching to each node by soldered taps with power-only USB-C connectors for the ESP32. We mounted each ESP32 inside a screw-lid plastic box with three sealed openings for the antenna, the shielded sensor cable, and the USB-C power cable.

Figure 3 shows our deployment steps. We marked excavation points with stakes and opened narrow cylindrical pits to the planned depth (Figure 3.a), softening compact layers with water when needed to preserve hole geometry. We verified depth with a ruler during excavation to ensure uniform sensor depth across sites. We installed the antennas and the reference probes so that the monopole and the capacitive sensor occupied the shallow root layer (Figure 3.b). We then backfilled and lightly compacted the soil while avoiding strain on cable terminations (Figure 3.c).

5. Results and Discussion

We present laboratory analyses of CSI sensitivity to localized moisture. We then report field evaluations of sensor range, amplitude and phase readings, given the architecture presented in Section 3.

5.1. Laboratory Experiment

Figure 4 shows the mean RSSI perceived by the STA across the irrigation steps described in Section 4.1. The link exhibits asymmetry: watering cells closer to the STA produced stronger signal attenuation. Additionally, in some steps, the RSSI increased with the increment of water. This behavior indicates propagation paths that bypass the soil (signal leakage) and arrive at the receiver with less attenuation, reaching outside the container. As a result, the CSI becomes influenced by the surrounding environment rather than solely by the soil between the devices.

These findings show that confined environments could introduce significant biases. The container enables alternative propagation paths with limited interaction with the

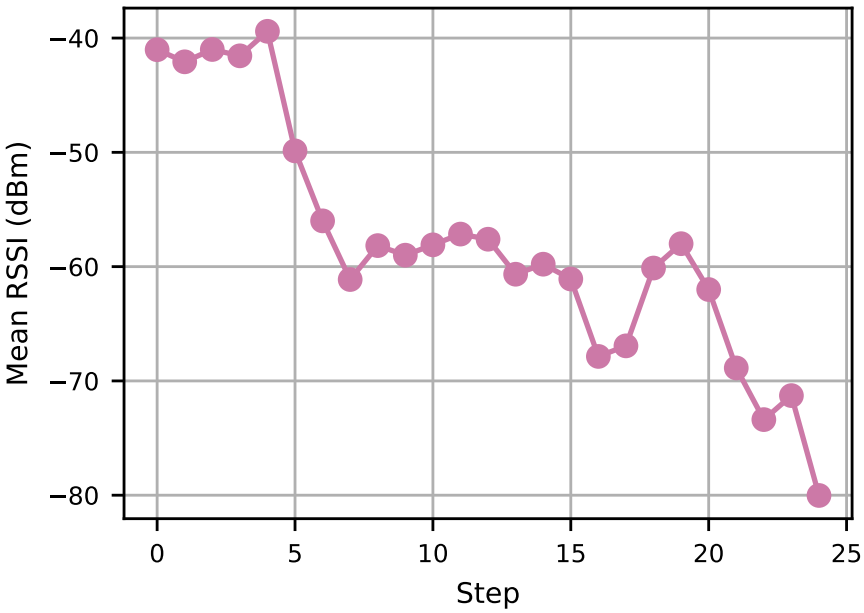

Figure 4. RSSI over watering steps.

soil. This effect compromises the interpretation of CSI as a direct indicator of moisture between the devices. Field experiments are therefore necessary to evaluate the technique under realistic conditions. In the outdoors scenario, propagation paths more accurately reflect the interaction between the signal and the soil.

5.2. Field Experiment

Regarding the field experiment, we conducted a 48-hour data collection run. We first evaluated the reliability of the chosen sensor distances by analyzing the sensing rate. We define the sensing rate as the ratio between the number of sensing frames received by a given sensor and the last sequence number generated by the initiator.

After aggregating the data from all sensors, we observed a lower sensing rate at nodes farther from the initiator. Figure 5.a shows the sensing rate for each sensor node in the experimental setup. This pattern indicates that increased soil moisture raises signal attenuation, preventing distant sensors from receiving frames and estimating CSI. Figure 5.b presents the mean RSSI for the sensed frames. Devices located more than 33 cm away receive mean power levels close to the microcontroller sensitivity threshold (-94 dBm) and may experience frame loss as soil moisture increases. This result suggests that practical deployments must consider limited sensing ranges when antennas are buried in moist soil.

As a result, we measured the amplitude and relative phase only for the first sensor (at 33 cm). We averaged points over one-minute windows (600 samples at 10 Hz) and calculated the aforementioned metrics for each subcarrier. The relative phase represents the phase shift from the first frame recorded. This is accomplished by unwrapping the phase of each subcarrier over time. Finally, we registered the moisture level (in mV) of the reference sensors of both the initiator and the sensor nodes.

Figure 6 plots the reference moisture, while Figure 7 shows the heatmap of the

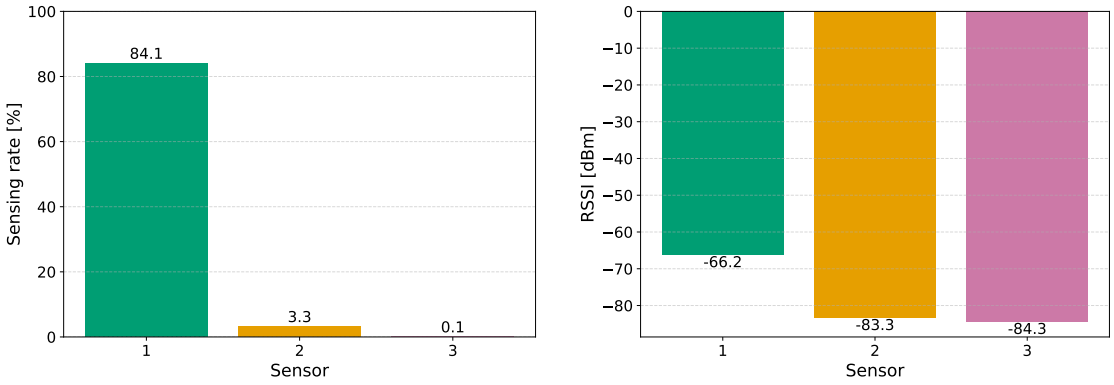

(a) Frame sensing rate.

(b) Sensor performance regarding distance from initiator.

Figure 5. Laboratory experiment setup.

channel metrics of interest. As moisture rises (lower probe voltage), amplitude decreases (Figure 7.a) while phase increases (Figure 7.b). After the 20-hour mark, the reference sensor registers higher local moisture (Figure 6), reflected primarily in lower-frequency subcarriers (indexes from -26 to -1). In this scenario, amplitude shows stronger correlation with moisture in the lower subcarriers, with its maximum at index -26 (coefficient of 0.55), whereas phase reaches its strongest correlation at a higher subcarrier, index 14 (coefficient of -0.58). This separation suggests that soil moisture does not influence the OFDM spectrum uniformly. Instead, the moisture-related response concentrates in specific subcarrier regions, which means that subcarrier selection matters for sensing performance.

The different correlation locations for amplitude and phase also indicate that the two metrics respond to moisture in distinct ways. Although the correlations remain moderate, the structured pattern across subcarriers shows that CSI captures measurable moisture sensitivity and that amplitude and phase provide complementary views of the same channel variation.

Considering an application scenario with scheduled irrigation, the nodes do not need to continuously generate or sense Wi-Fi frames. The initiator could generate sensing frames over a time window and repeat after some some time, depending on the needs of the crop and the expected moisture variation on soil (closer sensing windows around irrigation periods and less frequent windows hours after irrigation). This operation would require a coordination between the irrigation scheduler, the sensing initiator and the sensors on the same group. The initiator could inform its next sensing window to the sensors through the transmitted sensing frames (during a sensing window) or through the unburied antenna (on the allocated communication slot). In this scenario, entering a low-power mode and switching between sensing and communication antennas should be adjusted to this dynamic schedule.

6. Final Remarks

In this work, we evaluated Wi-Fi sensing and communication using ESP32 microcontrollers in laboratory and field conditions. Results show that confined setups bias channel

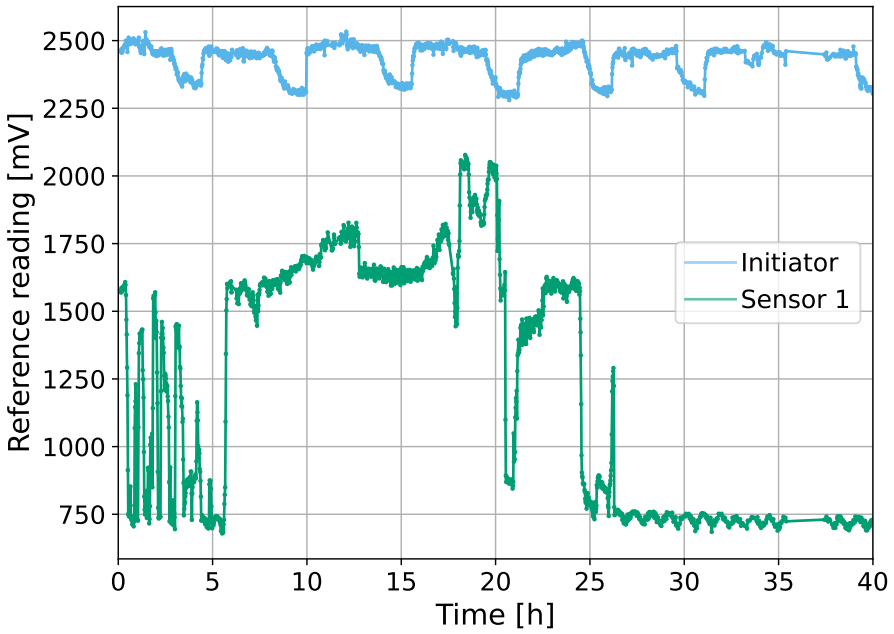

Figure 6. Reference moisture readings.

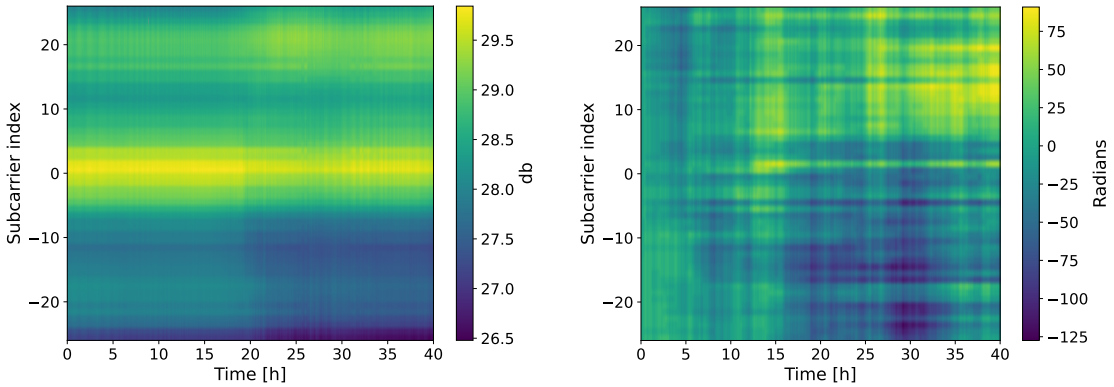

(a) OFDM amplitude.

(b) OFDM relative phase.

Figure 7. Channel (a) amplitude and (b) relative phase over time. After the 20-hour mark, the OFDM subcarriers show lower amplitude, with higher absolute relative phase.

metrics, field sensing degrades with range, and soil moisture affects signal amplitude and phase in complementary ways.

Future work should investigate the impact of soil texture by characterizing the soil sample under varying moisture conditions. Also, alternative sensor arrangements should be considered, including vertical alignment of transceivers (to profile the soil moisture layers) and external transmitters, such as a commercial router already present in the environment.

Acknowledgements

This study was financed in part by the Coordenação de Aperfeiçoamento de Pessoal de Nível Superior—Brasil (CAPES)—Finance Code 001. Cíntia Borges Margi is supported by CNPq fellowship #311687/2022-9. Henrique Freire da Silva is supported by CNPq fellowship #144334/2025-9.

We acknowledge the use of ChatGPT for assistance with text revision.

References

Chen, C., Song, H., Li, Q., Meneghello, F., Restuccia, F., and Cordeiro, C. (2023). Wi-Fi Sensing Based on IEEE 802.11bf. *IEEE Communications Magazine*, 61(1):121–127.

Cui, Y., Liu, F., Jing, X., and Mu, J. (2021). Integrating Sensing and Communications for Ubiquitous IoT: Applications, Trends, and Challenges. *IEEE Network*, 35(5):158–167.

Ding, J. and Chandra, R. (2020). Strobe: Towards low-cost soil sensing using wi-fi. *GetMobile: Mobile Comp. and Comm.*, 23(4):30–33.

Ding, J., Chandra, R., Lal, R., and Tassiulas, L. (2024). Cost-effective soil carbon sensing with wi-fi and optical signals. In *Proceedings of the 30th Annual International Conference on Mobile Computing and Networking*, ACM MobiCom '24, page 1015–1029, New York, NY, USA. Association for Computing Machinery.

Elshikha, D. E. (2024). Guidance for soil moisture sensor selection: Market analysis and decision-making strategies. University of Arizona Cooperative Extension, Publication AZ2082.

Espressif Systems (2026). Espressif product selector. Accessed: 2026-05-14.

Hardie, M. (2020). Review of novel and emerging proximal soil moisture sensors for use in agriculture. *Sensors*, 20(23).

Hernandez, S. M. and Bulut, E. (2023). Wifi sensing on the edge: Signal processing techniques and challenges for real-world systems. *IEEE Communications Surveys & Tutorials*, 25(1):46–76.

Hernandez, S. M., Erdag, D., and Bulut, E. (2021). Towards dense and scalable soil sensing through low-cost wifi sensing networks. In *2021 IEEE 46th Conference on Local Computer Networks (LCN)*, pages 549–556.

Hänel, T. and Kaiser, L. (2024). Estimating soil moisture with cots hardware using ble's angle-of-arrival feature. In *2024 IEEE 49th Conference on Local Computer Networks (LCN)*, pages 1–6.

IEEE (2021). Telecommunications and Information Exchange between Systems - Local and Metropolitan Area networks – Specific Requirements - Part 11: Wireless LAN Medium Access Control (MAC) and Physical Layer (PHY) Specifications. Technical Report 802.11, IEEE Standard for Information Technology.

Kashyap, B. and Kumar, R. (2021). Sensing Methodologies in Agriculture for Soil Moisture and Nutrient Monitoring. *IEEE Access*, 9:14095–14121. Conference Name: IEEE Access.

Kiv, D., Allabadi, G., Kaplan, B., and Kravets, R. (2021). smol: Sensing soil moisture using lora. In *Proceedings of the 1st ACM Workshop on No Power and Low Power Internet-of-Things*, LP-IoT'21, page 21–27, New York, NY, USA. Association for Computing Machinery.

Nguyen, T. V., Li, J., Mishra, D., and Seneviratne, A. (2023). Frequency-sensitive soil moisture profiling using wifi sensing. In *2023 Joint European Conference on Networks and Communications & 6G Summit (EuCNC/6G Summit)*, pages 641–646.

Rasheed, M. W., Tang, J., Sarwar, A., Shah, S., Saddique, N., Khan, M. U., Imran Khan, M., Nawaz, S., Shamshiri, R. R., Aziz, M., and Sultan, M. (2022). Soil moisture measuring techniques and factors affecting the moisture dynamics: A comprehensive review. *Sustainability*, 14(18).

Topp, G., Davis, J., and Annan, A. (1980). Electrical conductivity and dielectric constant of soils at radio frequencies. *Journal of the Soil Science Society of America*, 44(3):444–450.

United Nations (n.d.). Global issues: Population. `https://www.un.org/en/global-issues/population`. Last accessed 20 january 2026.

Wang, J., Chang, L., Aggarwal, S., Abari, O., and Keshav, S. (2020). Soil moisture sensing with commodity rfid systems. In *Proceedings of the 18th International Conference on Mobile Systems, Applications, and Services*, MobiSys '20, page 273–285, New York, NY, USA. Association for Computing Machinery.